Eur. Phys. J. E **12**, s01 (2003) 015
Digital Object Identifier (DOI) 10.1140/epjed/e2003-01-015-3

EPJ E direct
electronic only

Dynamics of supercooled water in mesoporous silica matrix MCM-48-S

A. Faraone[1,2], L. Liu[1], C.-Y. Mou[3], P.-C. Shih[3], C. Brown[4,5], J.R.D. Copley[4], R.M. Dimeo[4], and S.-H. Chen[1,a]

[1] Department of Nuclear Engineering, MIT, Cambridge, Massachusetts, USA
[2] Department of Physics and INFM, University of Messina, Messina, Italy
[3] Department of Chemistry, National Taiwan University, Taipei, Taiwan
[4] NIST Center for Neutron Research, Gaithersburg, Maryland, USA
[5] Department of Material Science and Engineering, University of Maryland, College Park, Maryland, USA

Received January, 2003
Published online November 5, 2003 © EDP Sciences / Società Italiana di Fisica / Springer-Verlag 2003

Abstract. Using three different quasielastic neutron spectrometers with widely different resolutions, we have been able to study the microscopic translational and rotational dynamics of water, in a mesoporos silica matrix MCM-48-S, from $T = 300$ K to 220 K, with a single consistent model. We formulated our fitting routine using the relaxing cage model. Thus, from the fit of the experimental data, we extracted the fraction of water bound to the surface of the pore, the characteristic relaxation times of the long-time translational and rotational decays, the stretch exponent describing the shape of the relaxation processes, and the power exponent determining the Q-dependence of the translational relaxation time. A tremendous slowing down of the rotational relaxation time, as compared to the translational one, has been observed.

PACS. 61.20.Lc Time-dependent properties of liquid structure; relaxation – 61.12.Ex Neutron scattering

1 Introduction

Understanding the microscopic dynamic behavior of water near hydrophilic surfaces is of fundamental interest both from a theoretical and practical point of view. In particular, the study of its temperature dependence, in the supercooled region, is believed to be the key for understanding its anomalous behavior [1]. In order to reach lower temperatures without freezing, water has been confined in nano porous sieves. Moreover it has been found that inside these nanometric pores the mechanisms for diffusion are altered.

In the past, we have studied the translational dynamics of water confined in pores of Vycor glass [2]. We are now collecting quasielastic neutron scattering (QENS) data on water confined in lab synthesized mesoporous MCM glasses. These molecular sieves have smaller pores with a narrower size distribution than vycor glass. Moreover, it is possible to synthesize MCM matrices with different and well defined structures. In this paper we report the results of our QENS study on water confined in MCM-48-S. This matrix has a bicontinuous cubic structure with an average pore diameter of 22 Å. Collecting data at $Q > 1$ Å^{-1}, and using a realistic model, developed with the help of molecular dynamics (MD) simulations [3], we investigated both translational and rotational dynamics. Because of the strong slowing down of water dynamics, with decreasing temperature, we used different instruments in different temperature ranges, from room temperature to the deeply supercooled region ($T = 220$ K).

2 Experiment

To synthesize MCM samples, zeolite seeds were prepared by mixing $NaAlO_2$, NaOH, fumed silica, TEAOH aqueous solution (20%), and water, stirring for 2÷5 h, then placing the solution in an autoclave at 100 °C for 18 h. A clear solution of nanoprecursors was obtained. MCM-48-S [4] was synthesized by reacting zeolite seeds with cetyltrimethylammonium bromide solution (CTAB) at 150 °C for 6÷24 h. Samples were then collected by filtration, washed with water, dried at 100 °C in an oven for 6 h, and calcined at 580 °C for 6 h. The molar ratios of the reactants $NaAlO_2$: SiO_2: NaOH: TEAOH: C_{16}TMAB: H_2O were 1:37-67:1.5-9:11-22:18.3:3000-3500. Using X-ray diffraction we found that the matrix was well ordered with cubic (Ia3d) symmetry (see Fig. 1). Pore diameters were determined using a Nitrogen adsorption technique. MCM-48-S exhibits high hydrothermal stability. In order to hydrate the matrix we put the calcined samples to the diskette that was full of water vapor by pumping the saturated NaCl solution for 2–3 days. We thus obtained water-loaded samples with hydration levels of ≈35%. The

[a] e-mail: sowhsin@mit.edu

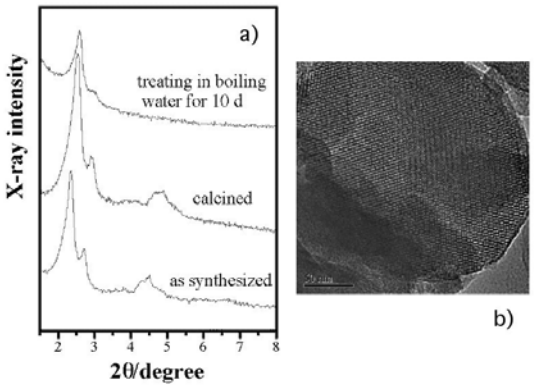

Fig. 1. The X-ray diffraction patterns (a) and transmission electron microscopy micrograph (b) of MCM-48-S.

amount of loading was determined by thermogravimetric analysis.

For the QENS experiment the hydrated powder was evenly spread to form a rectangular slab sample 0.5 mm thick, such that multiple-scattering corrections should not be necessary (transmission 95%).

The QENS measurements were carried out at the NIST Center for Neutron Research using the Fermi chopper (FCS), the disk chopper (DCS) and the backscattering (HFBS) spectrometers. For FCS and DCS the incident neutron wavelength was 6.0 Å and the gaussian energy resolution function had a Full Width at Half Maximum (FWHM) of ∼60 μeV and ∼30 μeV respectively. For HFBS we have chosen the low resolution configuration, corresponding to a resolution function with FWHM of ∼1.0 μeV and an energy window of ±36 μeV. In all cases, the rectangular sample cell was placed at 45° to the direction of the incident neutron beam. The detectors facing the edge of the can have been discarded. The resulting range of elastic wave-vector Q was from 0.33 Å^{-1} to 1.93 Å^{-1}, from 0.27 Å^{-1} to 1.93 Å^{-1}, and from 0.25 Å^{-1} to 1.60 Å^{-1}, in the case of FCS, DCS, and HFBS respectively. These Q ranges are broad enough to simultaneously monitor both translational and rotational dynamics of the water molecules.

3 Results and discussion

We analyzed QENS data using the relaxing cage model (RCM), which we developed using concepts introduced by Mode Coupling Theory (MCT). It has been tested against MD simulations [5,3] and has given good results when used to analyze QENS data of water in hydrated cement paste [6,7]. At supercooled temperatures, at short times, a water molecule is trapped inside the cage of its neighbors. Inside the cage, it performs harmonic vibrations and librations. For times longer than 0.1 ps the cage starts to relax and the water molecule may escape. Since this process is related to the cooperative motion of many molecules it could be described by a stretched exponential function. Thus, the RCM expresses the translational intermediate scattering function (ISF) of a water molecule as the product of a short time gaussian part and a long time stretched exponential: $F_T(Q,t) = F_T^s(Q,t)\exp\left[-(t/\tau_T)^\beta\right]$.

The short time part, F_T^s, is related to the translational part of the vibrational density of states, $Z_T(\omega)$. According to experiment [8] and simulations [5], $Z_T(\omega)$ has two peaks centered at ∼10 meV and ∼30 meV respectively. Taking into account these findings the RCM expresses the short time part of the translational ISF as:

$$F_T^s(Q,t) = \exp\left\{-Q^2v_0^2\left[\frac{1-C}{\omega_1^2}\left(1-e^{-\omega_1^2t^2/2}\right)+\frac{C}{\omega_2^2}\left(1-e^{-\omega_2^2t^2/2}\right)\right]\right\} \quad (1)$$

where $v_0 = \sqrt{k_BT/m}$ is the thermal speed of the water molecule, ω_1 and ω_2 the peak frequencies of the translational density of states of the hydrogen atom, and C expresses their relative weights.

The long time dynamics is characterized by a structural relaxation time, τ_T, which was shown to follow a power law in Q, namely, $\tau_T = \tau_0(aQ)^{-\gamma}$ [6,9]. Here a is a suitable length scale, the root mean square vibrational amplitude of water rattling inside the cage, defined by the long time limit of $F_T^s(Q,t)$. According to MD simulations $a = 0.5$ Å, and is fairly insensitive to temperature variations [5]. The exponent γ is two for simple diffusion, in this case τ_T is connected to the translational diffusion coefficient by the relation $D = a^2/\tau_0$. In confinement it has been often found that γ is less than two [9]. Finally the parameter β can be considered Q independent [7] in the Q range investigated.

The two-step relaxation process applies to the rotational dynamic as well. Thus, the first order rotational correlation functions, $C_1(t)$, can be described as the product of a short time part and a stretched exponential: $C_1(t) = C_1^s(t)\exp\left[-(t/\tau_R)^\beta\right]$.

The short time part, C_1^s, describing the libration of water in the cage, is related to the rotational part of the vibrational density of states, $Z_R(\omega)$ [3]. This is a broad band centered at around ∼65 meV. Thus, we expressed C_1^s by an empirical pseudo gaussian form that is able to reproduce $Z_R(\omega)$ from MD results and experiments with good accuracy:

$$C_1^s(t) = \exp\left\{-\frac{4\langle\omega^2\rangle}{45\omega_3^2}\left[3\left(1-e^{\frac{-\omega_3^2t^2}{2}}\right)+6\omega_3^2t^2e^{\frac{-\omega_3^2t^2}{2}}-\omega_3^4t^4e^{\frac{-\omega_3^2t^2}{2}}\right]\right\} \quad (2)$$

where $\langle\omega^2\rangle$ is the mean square angular velocity, related to the effective moment of inertia of the water molecule in the cage and ω_3 is the characteristic frequency of hindered rotations around the H-bond direction.

Because of the translational rotational coupling, the long time part of $C_1(t)$ coincides with the long time part of the translational ISF at a fixed Q^* value, as it has been shown using MD simulations [10]. Thus we use the same

stretch exponent for the long time translational and rotational decays. Then, by imposing the equality $\tau_T(Q^*) = \tau_R$, we were able to determine Q^*. Using the maximum entropy method [11], we determine the higher order rotational correlation functions from $C_1(t)$. Then we use the Sears expansion [12] to determine the rotational ISF from the rotational correlation functions. Finally, we adopt the decoupling approximation to obtain the hydrogen atoms' ISF, F_H, from the product of the translational, F_T, and rotational, F_R, ISFs: $F_H(Q,t) = F_T(Q,t) \cdot F_R(Q,t)$. It is important to say that we are not suggesting a statistical indipendence of the translational and rotational dynamics. However, the decoupling approximation is still able to reproduce F_H with sufficient accuracy when F_T and F_R are modeled correctly. In fact this approximation resulted valid within 10%, when tested against MD simulations of bulk water [3,13].

Performing an experiment on water confined in a silicate matrix, we expect that the neutron spectra originate from the contribution of i) the (non-hydrogenous) matrix; ii) the water molecules bound to the surface of the sieves; iii) the water molecules in the inner part of the pores. The first two contributions give rise to an elastic component [14], and the latter accounts for the quasielastic broadening. Thus:

$$S(Q,\omega) = pR(Q_0,\omega) + (1-p)FT\{F_H(Q,t)R(Q_0,t)\} \quad (3)$$

where, p is the fraction of elastic scattering, $E = \hbar\omega$ is the energy transfer of the neutron, and Q is the magnitude of the wavevector transfer corresponding to this energy transfer at the scattering angle θ. $R(Q_0,t)$ is the Fourier transform of the experimental resolution function, $R(Q_0,\omega)$. Since the model contains only Q-independent parameters, p, τ_0, γ, τ_R, β, we fit the experimental $S(Q,\omega)$ surface. Thus we succeded analyzing 7, 9, and 11 spectra with the same 5 fitting parameters for every HFBS, DCS, and FCS run respectively. The short time part of the translational ISF and first order rotational correlation function, F_T^s and C_1^s, have been fixed according to the results of MD simulations [3,5], which agree with previous inelastic neutron scattering measurements [8]. Since the elastic Q is less than 2, just the first three terms of the Sears expansion have been used.

In Figure 2 we show, as an example, the experimental spectra at $T = 230$ K (HFBS), 260 K (DCS), and 300 K (FCS), at $Q \simeq 1.5$ Å^{-1}. In the figure we show also the results of the fit and the first three terms of the Sears expansion, namely $FT\{j_0^2 F_T \cdot R\}$, $FT\{3j_1^2 F_T \cdot C_1 \cdot R\}$, $FT\{5j_2^2 F_T \cdot C_2 \cdot R\}$. The good quality of the fit ensures that the model is able to describe the experimental data.

In Figure 3 we report the resulting fitting parameters as a function of temperature. In plot a) we show the weight of the elastic component. At high temperatures it tends to a limiting value (∼0.10), which we interpret as the contribution from the glass matrix. The value of p increases with decreasing temperature, showing that the fraction of water molecules immobile on the QENS time scale increases. However, we can still resolve a quasielastic broadening at $T = 220$ K. The stretching exponent, β,

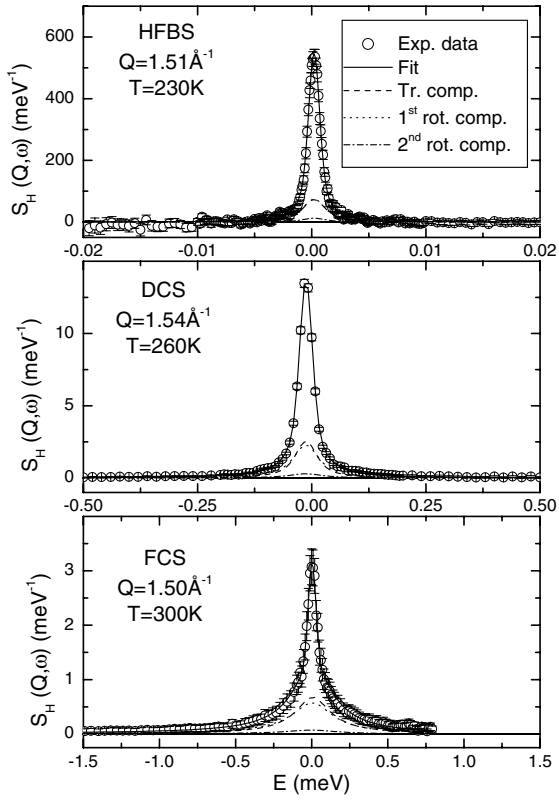

Fig. 2. Typical QENS spectra from the MCM-48-S sample at three different temperatures, with the three spectrometers. The continuous, dash, dot, and dash-dot lines represent the total fit and the contributions from the first three terms of the Sears expansion respectively.

is less than 1 at high temperatures, indicating that both translational and rotational relaxation processes are non-exponential. However, it increases with decreasing temperature, and at low temperature we find $\beta = 1$. This result might be due to the nonzero resolution of the instrument that, as the dynamics slows down, is not able to fully resolve the non-Lorentzian feature of the spectra. Lowering temperature seems to strongly affect the dimensionality of the diffusion process, that is more and more hindered, as shown by the decrease of the exponent γ. It is remarkable that $\gamma = 2$ at high temperature, as it is expected for a diffusive process. In this case we can evaluate the translation diffusion constant for a direct comparison with the values reported for bulk water. We use the average translational relaxation time, $\langle\tau_T\rangle = \frac{\tau_0}{\beta}\Gamma(1/\beta)$, to take into account the non exponentiality of the process, $D = a^2/\langle\tau_T\rangle = 1.06 \times 10^{-5}$ cm^2/s and $D = 7.06 \times 10^{-4}$ cm^2/s, at $T = 300$ K and $T = 290$ K respectively. These values are much smaller than those reported in reference [15] for bulk water, $D = 2.41 \times 10^{-5}$ cm^2/s at $T = 300$ K and $D = 1.87 \times 10^{-5}$ cm^2/s at $T = 290$ K. This finding shows that inside these nanometric pores the translational dynamic is strongly slowed down already at room temperature.

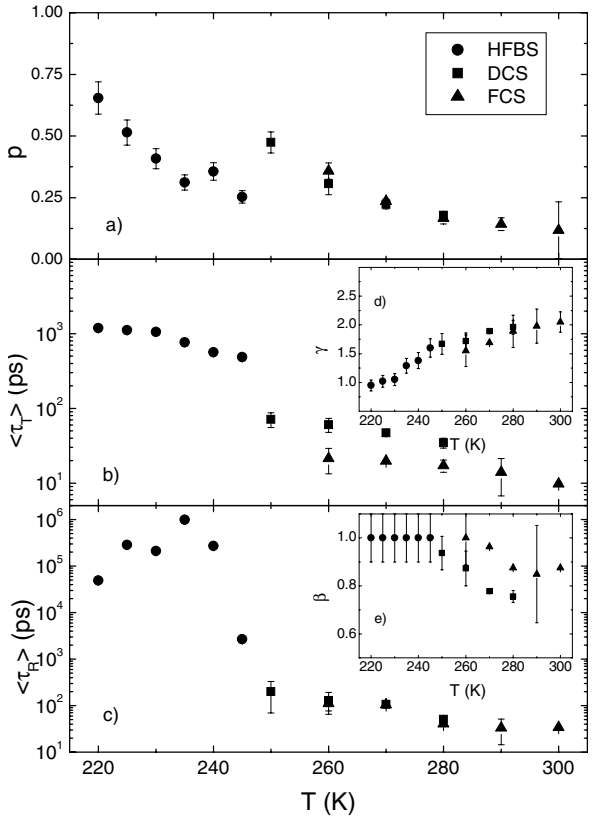

Fig. 3. Temperature dependence of the resulting fitting parameters. In panel c) note the tremendous slowing down of the rotational relaxation time upon supercooling.

Plot b) and c) show the logarithmic increase of the average translational and rotational relaxation times, $\langle\tau_T\rangle$ and $\langle\tau_R\rangle = \frac{\tau_R}{\beta}\Gamma(1/\beta)$ respectively. Please, note that the values of τ_0 and τ_R span 3 orders of magnitude in time. The use of different spectrometers with different resolutions was absolutely necessary to appreciate this dramatic slowing down. Nevertheless, the values of $\langle\tau_T\rangle$ obtained with the different instruments do not perfectly agree. This is possibly due to the fact that the extracted value of $\langle\tau_T\rangle$ is lower than its effective value when it is close to the limit of the resolution of the instrument. Thus, it is possible that the values obtained using FCS at $T \leq 280$ K, and DCS at ≤ 260 K are underestimated.

As far as the rotational dynamics is concerned, we believe that at temperature lower than $T = 240$ K, the rotational decay is too slow to be determined with the HFBS resolution of 1 μeV. We still observe a dramatic slowing down of the rotational dynamics. We tentatively analyzed these data using a critical law fit, $\tau_R = \tau_R^0(T/T_c - 1)^{-\delta}$. We have found that this formula describes the data from $T = 300$ K to $T = 240$ K, with fair accuracy, where $\tau_R^0 = 7.89$ ps, $T_c = 243.8$ K, $\delta = 0.95$. The study of this issue is still preliminary, however we find this result quite interesting and worthy of investigation.

Table 1. Extracted values of Q^*.

Q^* (Å^{-1})	HFBS	DCS	FCS
$T = 245$ K	0.34 ± 0.13	-	-
$T = 250$ K	-	0.54 ± 0.29	-
$T = 260$ K	-	0.64 ± 0.25	0.34 ± 0.27
$T = 270$ K	-	0.65 ± 0.05	0.37 ± 0.24
$T = 280$ K	-	0.82 ± 0.15	0.63 ± 0.27
$T = 290$ K	-	-	0.64 ± 0.43
$T = 300$ K	-	-	0.54 ± 0.15

In Table 1 we report the extracted values of Q^* from the relation: $Q^* = \frac{1}{a}(\tau_0/\tau_R)^{1/\gamma}$. We discarded the Q^* values for $T \leq 240$ K because the values of τ_R are not reliable, however, as shown in Figure 3, the other fitting parameters are reliable in the whole T range. The obtained values lie between 0.35 and 0.65 Å^{-1}, without a clear trend with temperature. This finding supports the MD result that Q^* is temperature independent [10]. However the experimental value seem smaller than the one obtained from MD simulations of bulk water, $Q^* = 0.8$ Å^{-1}.

4 Conclusion

We have investigated the single particle dynamics of water confined in a 3-D bicontinuous structure, with pore diameter of 22 Å, in an ample temperature range from 220 K to 300 K. We detected the power-law like slowing down of both the translational and rotational relaxation times, and we found that on lowering temperature the dimensionality of the diffusive process is strongly reduced.

Research at MIT is supported by DE-FG02-90ER45429 and 2113-MIT-DOE-591. This work utilized facilities supported in part by the National Science Foundation under Agreement No. DMR-0086210.

References

1. R.J. Speedy *et al.*, J. Chem. Phys. **65**, 851 (1976)
2. J.M. Zanotti *et al.*, Phys. Rev. E **59**, 3084 (1999)
3. L. Liu *et al.*, Phys. Rev. E **65** 041506 (2002)
4. P.-C. Shih *et al.*, Chem. Mater., submitted (2002)
5. S.-H. Chen *et al.*, Phys. Rev. E **59**, 6708 (1999)
6. E. Fratini *et al.*, Phys. Rev. E **64**, 020201 (2001)
7. A. Faraone *et al.*, Phys. Rev. E **65**, 040501 (2002)
8. M.-C. Bellissent-Funel *et al.*, Phys. Rev. E **51**, 4558 (1995)
9. V. Crupi *et al.*, J. Phys. Chem. B **106**, 10884 (2002)
10. L. Fabbian *et al.*, J. non-cryst. Sol. **235-237**, 325 (1998)
11. B.J. Berne *et al.*, J. Chem. Phys. **49**, 3125 (1968)
12. V.F. Sears, Can. J. Phys. **45**, 237 (1967)
13. S.-H. Chen *et al.*, Phys. Rev. E **56**, 4231 (1997)
14. P. Gallo *et al.*, Phys. Rev. Lett. **85**, 4317 (2000); J. Chem. Phys. **113**, 11324 (2000)
15. F.X. Preielmeier *et al.*, Phys. Chem. **92**, 1111 (1988)